

Determination of Temperature profile of Continuous Wave Ultraviolet Laser Induced LiNbO₃ Waveguide

T.Ghosh¹, B.Samanta², P.C.Jana¹, and P. Ganguly³

¹ Department of Physics and Technophysics, Vidyasagar University, Midnapur, 721102, India

² Department of Physics, Panskura banamali College, Panskura, 721152, India

³ Advanced Technology Development Centre, Indian Institute of Technology, Kharagpur, 721302, India

¹Email: sfortapas@gmail.com

Received October 19, 2012; accepted December 18, 2012

ABSTRACT

The temperature distribution of continuous wave UV written LiNbO₃ waveguides at 244 nm and 275 nm writing laser wavelengths are determined as a function of writing parameters. The model is used to determine the optimized writing parameters to keep the maximum temperature below the melting point (1257°C) of LiNbO₃ to avoid surface damage.

Keywords: LiNbO₃, UV-written waveguide, temperature profile, continuous wave.

1. Introduction

LiNbO₃ is a well known technologically important single crystal material because of its high electro-optic, piezoelectric, photorefractive, acousto-optic and nonlinear-optic effects. The continuous wave (CW) direct UV written waveguides in lithium niobate (LiNbO₃) has held considerable promise due to its easy single-step fabrication process, well suited for complex micro-optical components, apart from conventional optical integrated circuits. Direct writing of graded index channel waveguides in congruent z-cut LiNbO₃ has been demonstrated using CW laser light within a writing wavelength range of 244-305 nm [1-4]. The process has been identified as a laser induced thermal diffusion of lithium ions at the shorter wavelengths (244 & 275 nm). The Li-deficiency increases the extraordinary refractive index which guides light by total internal reflection. At wavelengths nearer to the left-edge of LiNbO₃ transmission window, where the absorption

coefficients are relatively low, the waveguiding process may be due to H-ion redistribution within the light irradiated region because of photorefractive effect and subsequent thermal fixing [5]. Since the UV laser induced temperature profile is the most important parameter for these waveguides, it has to be determined accurately. The modeling of temperature profile induced by laser radiation in solid was reported by a number of researchers [6-9] for stationary and moving laser beam. For accurate determination of temperature profile, the temperature dependent thermal diffusivity has been introduced [10]. They have assumed no light penetration into the irradiated material for moving beam and hence their temperature profile is a function of laser spot size only. Temperature distribution was further investigated as a function of incident power and beam spot size [11].

In the present work the effects of writing parameters on the laser induced temperature profile of congruent LiNbO₃ crystal is studied for 244 and 275 nm writing wavelengths where the absorption coefficients are relatively high and considered uniform throughout the crystal. The temperature dependent thermal diffusivity of the substrate has also been taken into account. The absolute values of the laser induced temperature of the crystal sets the refractive index distribution of the crystal and its usefulness in integrated-optic applications. The results of the computations for realistic waveguide writing parameters are discussed in section-3, and finally the work is concluded in section-4.

2. Theory

We have considered the co-ordinates x , y and z attached to static reference frame of the z -cut crystal, while $X = \frac{x-vt}{w}$, $Y = \frac{y}{w}$ and $Z = \frac{z}{w}$ corresponds to reference frame attached with the moving laser beam as shown in fig-1.

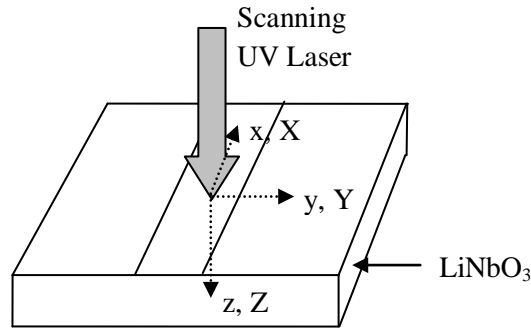


Figure 1: Schematic of the scanning laser beam.

Determination of Temperature profile of Continuous Wave Ultraviolet Laser
Induced LiNbO₃ Waveguide

The heat source, $S(\vec{r}, t)$, is the scanning Gaussian UV laser beam which is absorbed within LiNbO₃ near the surface and converted into heat through photon relaxation. The heat equation in the isotropic case can be written as [11]

$$\frac{\partial T}{\partial t} - \nabla \cdot D(T) \nabla T = \frac{1}{\rho C_v} S(\vec{r}, t) \quad (1)$$

where ρ is the density of LiNbO₃, C_v is the specific heat at constant volume, T is the temperature in absolute scale, t is time, and $D(T)$ is thermal diffusivity tensor. The temperature dependent thermal diffusivity $D(T)$ can be replaced by Kirchhoff transformation using the assumption of constant ρC_v .

We may write Kirchhoff transformation as [11]

$$\theta(T) = \theta(T_0) + \frac{1}{D(T_0)} \int_{T_0}^T D(T') dT' \quad (2)$$

Where θ is the new temperature variable and $D(T_0)$ is the thermal diffusivity at the temperature T_0 . The value of $\theta(T_0)$ is assumed to be zero. The equation (1) may be expressed in terms of new temperature variable in moving frame as

$$\frac{vw}{D(T(\theta))} \frac{\partial \theta}{\partial X} - \nabla^2 \theta = \frac{w^2 S(X, Y, Z)}{D(T_0) \rho C_v} \quad (3)$$

Where w is the spot radius. It may be shown that in all practical cases of waveguide writing laser scanning speed $v \ll D(T)/w$, which yields

$$\nabla^2 \theta = - \frac{w^2 S(X, Y, Z)}{D(T_0) \rho C_v} \quad (4)$$

The above equation may be regarded as Poisson's equation and may be expressed as

$$\nabla^2 G = -\delta(\vec{r} - \vec{r}') \quad (5)$$

Where Green's function $G(\vec{r}, \vec{r}')$ may be written in terms of Fourier transform

$g(\vec{r}', \vec{k})$ as

$$G(\vec{r}, \vec{r}') = \frac{1}{(2\pi)^{3/2}} \int_{-\infty}^{\infty} g(\vec{r}, \vec{k}) \exp(i\vec{k} \cdot \vec{r}) d\vec{k} \quad (6)$$

Substituting the value of $G(\vec{r}, \vec{r}')$ in equation (5) one obtains

$$g(\vec{r}, \vec{k}) = \frac{1}{(2\pi)^{3/2} k^2} \exp(-i\vec{k} \cdot \vec{r}) \quad (7)$$

Now from equation (6) and (7) we have

$$G(\vec{r}, \vec{r}') = \frac{1}{(2\pi)^3} \int_{-\infty}^{\infty} \frac{1}{k^2} \exp[i\vec{k} \cdot (\vec{r} - \vec{r}')] d\vec{k} \quad (8)$$

$$\theta = \int_{-\infty}^{\infty} G(\vec{r}, \vec{r}') \frac{w^2 s(r')}{\rho C_v D(T_0)} d\vec{r}'$$

Substituting the value of $G(\vec{r}, \vec{r}')$ in above equation and rearranging we may rewrite as

$$\theta(X, Y, Z) = \frac{A}{2\pi^2} \iiint_{-\infty}^{\infty} \iiint \frac{S(X', Y', Z')}{(k_1^2 + k_2^2 + k_3^2)} \times \exp[i\{k_1(X - X') + k_2(Y - Y') + k_3(Z - Z')\}] dX' dY' dZ' dK_1 dk_2 dk_3 \quad (9)$$

$$\text{Where } k^2 = k_1^2 + k_2^2 + k_3^2 \text{ and } A = \frac{w^2}{4\pi\rho C_v D(T_0)}$$

In order to solve equation (9) we have introduced the expressions

$$\frac{1}{r} = \int_0^{\infty} \exp(-r\lambda) d\lambda \quad (10)$$

$$S(X', Y', Z') = B \exp[-2(X'^2 + Y'^2)] \exp(-\alpha w |Z'|) \quad (11)$$

$$B = \frac{2p(1-R)\alpha}{\pi w^2} \quad (12)$$

where p is the incident laser power, R is the reflection coefficient of the laser beam from LiNbO₃ surface, and α is the absorption coefficient of the laser light in the material.

Using equations (9-12) and rearranging we have

$$\theta(X, Y, Z) = 4AB\sqrt{\pi} \int_{-\infty}^{\infty} \int_0^{\infty} \frac{1}{\sqrt{\lambda}} \times \frac{1}{2+16\lambda} \exp[-2(\frac{X^2 + Y^2}{1+8\lambda})] \times \exp[-\alpha w |Z'| - \frac{(Z-Z')^2}{4\lambda}] dZ' d\lambda$$

Z' integral can evaluated as follows.

Determination of Temperature profile of Continuous Wave Ultraviolet Laser
Induced LiNbO₃ Waveguide

$$\int_{-\infty}^{\infty} \exp[-\alpha w |Z'| - \frac{(Z-Z')^2}{4\lambda}] dZ',$$

$$= \exp[-\frac{Z^2}{4\lambda}] \int_0^{\infty} \exp[-\frac{Z'^2}{4\lambda} - Z'(\alpha w + \frac{Z}{2\lambda})] dZ' + \exp[-\frac{Z^2}{4\lambda}] \int_0^{\infty} \exp[-\frac{Z'^2}{4\lambda} - Z'(\alpha w - \frac{Z}{2\lambda})] dZ'$$

These may be expressed in the form of error function as

$$\int_0^{\infty} \exp(-az^2 - bz) dz = \frac{1}{2} \sqrt{\frac{\pi}{a}} \exp(\frac{b^2}{4a}) \operatorname{erfc}(\frac{b}{2\sqrt{a}})$$

Hence Z' integral becomes

$$\sqrt{\pi\lambda} \exp(-\frac{Z^2}{4\lambda}) \{ \exp[(\alpha w - \frac{Z}{2\lambda})^2 \lambda] \operatorname{erfc}[(\alpha w - \frac{Z}{2\lambda})\sqrt{\lambda}] + \exp[(\alpha w + \frac{Z}{2\lambda})^2 \lambda] \operatorname{erfc}[(\alpha w + \frac{Z}{2\lambda})\sqrt{\lambda}] \}$$

$$= \sqrt{\pi\lambda} h(Z, \lambda)$$

Substituting the value in equation (13) we rewrite as[11]

$$\theta(X, Y, Z) = \frac{p(1-R)}{\pi\rho c_v D(T_0)} \int_0^{\infty} \frac{1}{1+8\lambda} g(X, Y, \lambda) h(Z, \lambda) d\lambda \quad (14)$$

$$\text{where } g(X, Y, \lambda) = \exp[-\frac{2(X^2 + Y^2)}{1+8\lambda}]$$

The numerical solution of equation (14) is obtained by accurately choosing the limit of integration. To get a solution for temperature in terms of T, the same Kirchhoff transform is used again along with an empirical relation between D(T) and T, which yields [11]

$$T(\theta) = T_0 \exp(\frac{\theta}{T_0}) \quad (15)$$

One can determine the temperature distribution due to UV laser light during waveguide writing process by solving eq.(14) numerically. Our interest in this work is to estimate the maximum temperature (which will occur at time t = 0) during the writing process and that temperature should be below the melting point (1257°C) of LiNbO₃ to avoid the local damage of the waveguide. The surface damage of the UV laser written waveguide will result in higher propagation loss at the transmitting wavelength.

3. Results and discussions:

The computed temperature profiles along y and z direction for a fixed spot radius (2 μm) and different laser powers are shown in Fig.1 and Fig.2 respectively for 244

nm wavelength. It may be observed that for 21.35 mw power the peak temperature is 1257°C, melting point of LiNbO₃ and it decreases with decreasing power. It is also observed that the curves are more steeper in z direction with respect to the y direction. It implies that light is absorbed more rapidly in z direction.

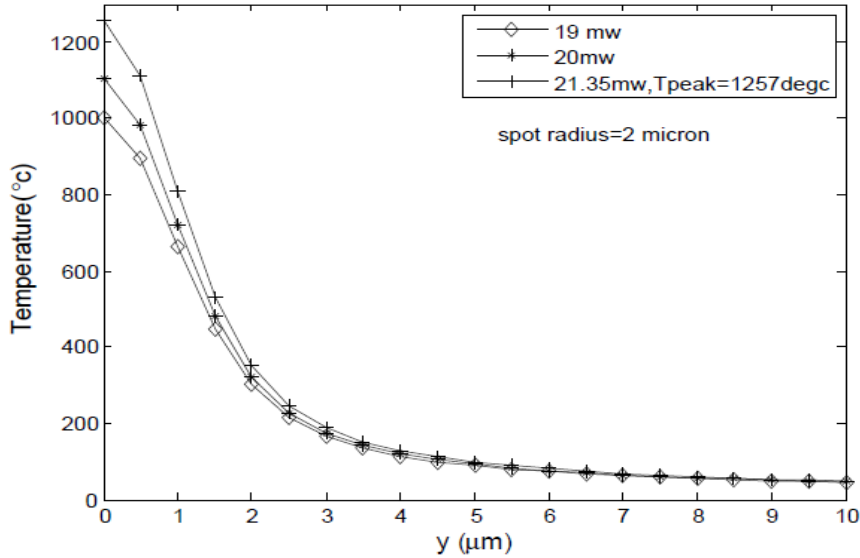


Figure 2: Initial temperature profile of waveguide at 244 nm along y direction

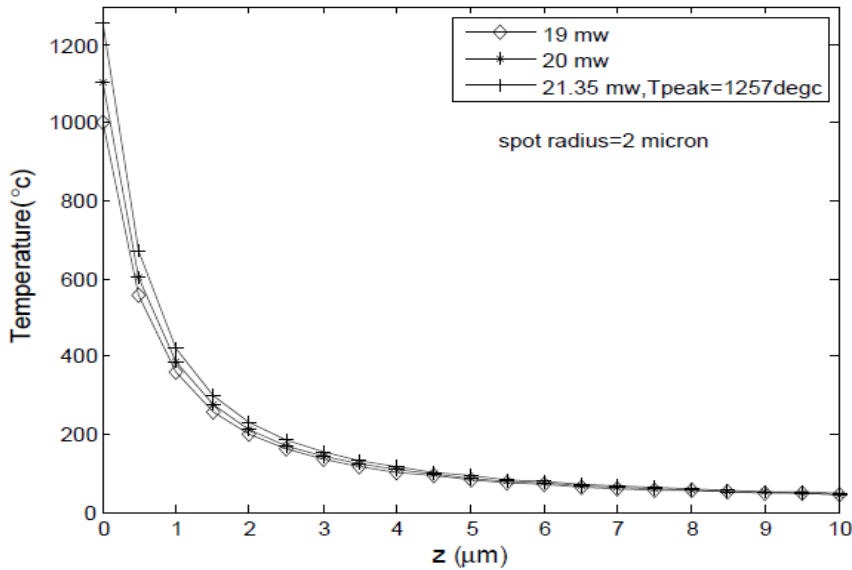


Figure 3: Initial temperature profile of waveguide at 244 nm along z direction

Determination of Temperature profile of Continuous Wave Ultraviolet Laser Induced LiNbO₃ Waveguide

The determination temperature profile at 2 μm spot radius with different laser powers along y and z directions for 275 nm wavelength of writing laser is shown in fig.4 and fig.5. It is noticed that the peak temperature is 1257°C at 30.15 mw writing power. From temperature profile for 244 nm and 275 nm we may conclude that for fixed spot radius the higher power is required at higher wavelength to reach the same peak temperature. It may also be noticed that half width at half maxima increases at 275 nm wavelength. It is observed that z profile at 275 nm is less steep than that at 244 nm. This implies that total diffused heat is absorbed by a larger volume for writing wavelength at 275 nm compare to that at 244 nm.

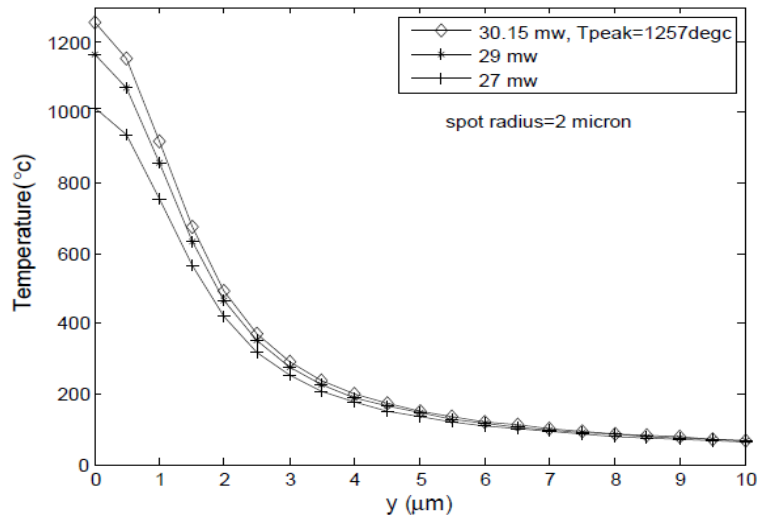


Figure 4: Temperature profile of LiNbO₃ waveguide along y direction at 275 nm wavelength laser.

Temperature profiles are also computed for different beam radii at constant beam power and it may be pointed out that maximum temperature remains below 1257°C for spot radius of 2.159 μm and above, for a writing power of 23 mw at 244nm wavelength. The computations are also repeated for 275 nm writing wavelength and the variation of maximum temperature with beam power for different spot radii are compared with 244 nm in Fig.6 and Fig.7. It has been observed that the maximum allowable power for 275 nm is ~30 mw for 1.985 μm spot radius.

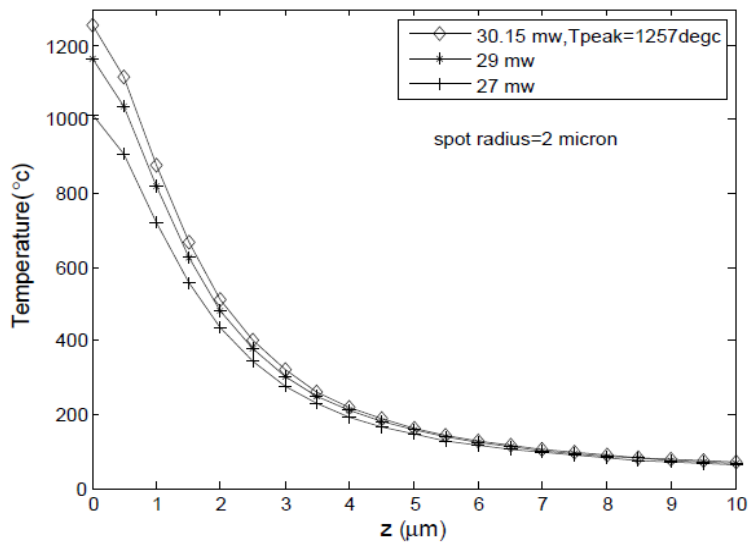


Figure 5: Temperature profile along z direction at 275 nm wavelength of writing laser source.

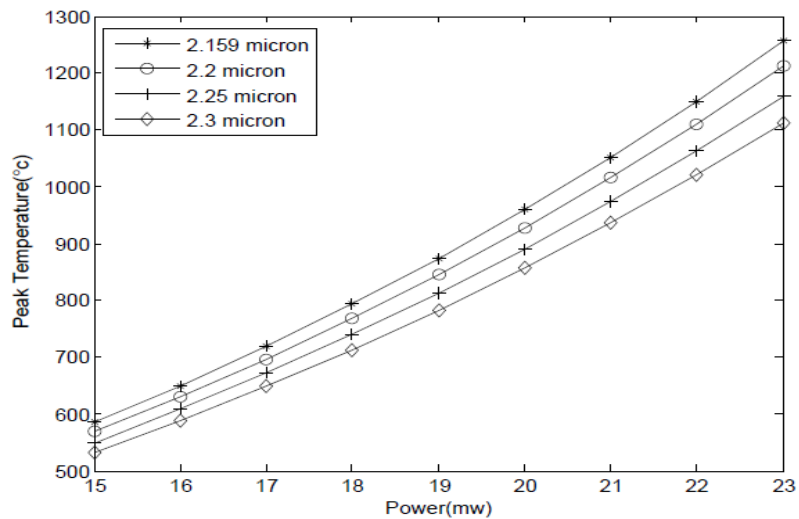


Figure 6: Variation of peak temperature with laser power at 244 nm

Determination of Temperature profile of Continuous Wave Ultraviolet Laser Induced LiNbO₃ Waveguide

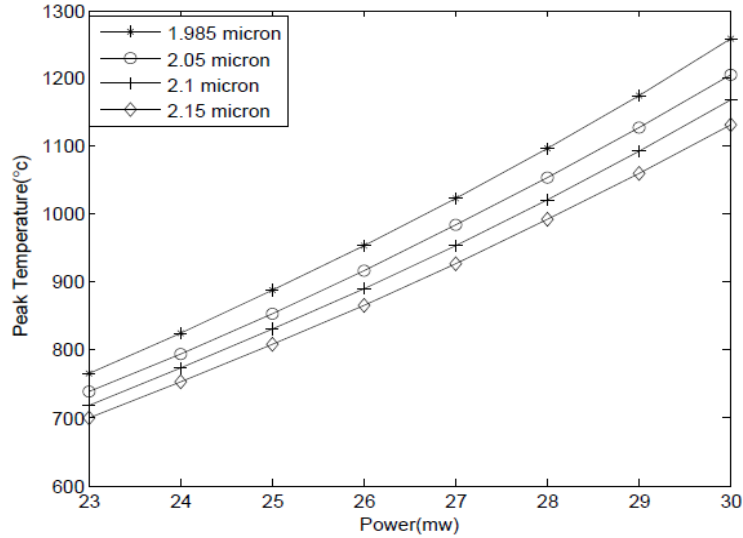


Figure 7: Variation of peak temperature with laser power at 275 nm

The fig.8 and fig.9 show that at initial time($t=0$) the peak temperature is maximum (1257°c) for 21.35 mw power and 2 μm spot radius and it decreases with time. The peak temperature decreases with time due to gradual movement of laser spot away from the determination point. The values of the physical constants used in the temperature distribution model of the UV-written waveguides are listed in Table-1

4. Conclusion

The laser induced temperature distributions during the writing process of CW direct UV-written waveguides in congruent LiNbO₃ crystal are computed from the writing laser parameters. The laser powers and its spot sizes are optimized at 244 nm and 275 nm wavelengths to avoid temperature induced optical damage. The process may also be used to determine the writing parameters of the waveguide so that the maximum temperature of the crystal during laser exposure is below the Curie temperature (1144°C), which results into electro-optically active LiNbO₃ waveguides.

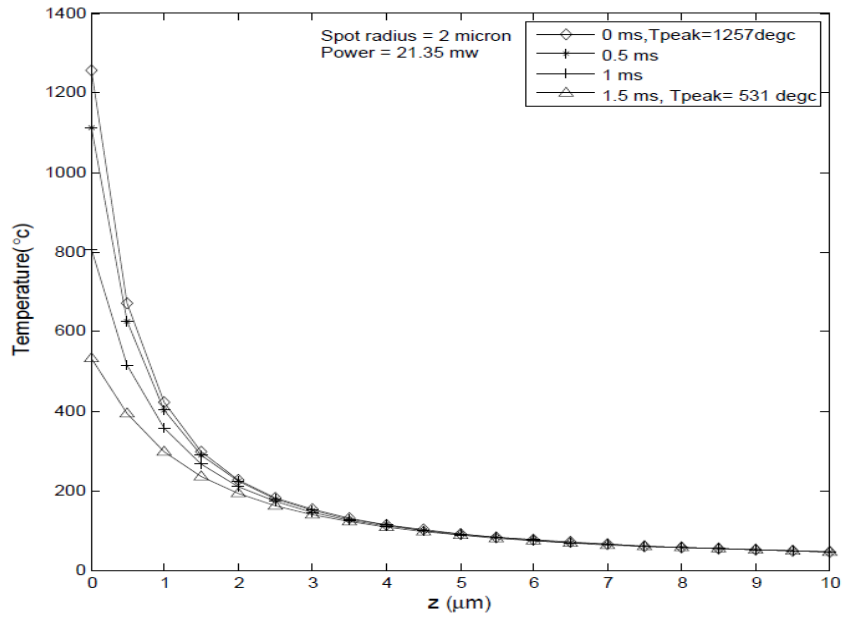


Figure 8: Temperature profile along z for fixed power and spot radius with different time instants after exposure to laser

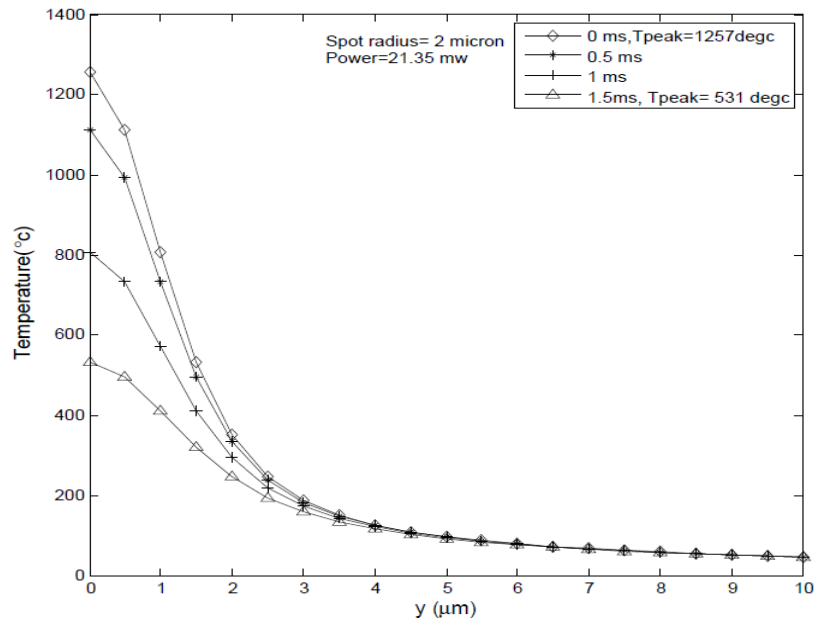


Figure 9: Temperature profile along y for fixed power and spot radius at different time instants after exposure to laser

Determination of Temperature profile of Continuous Wave Ultraviolet Laser
Induced LiNbO₃ Waveguide

Table 1: Used physical constants of LiNbO₃ in temperature distribution model

R	ρ (Kg/m ³)	C _v (J/Kg.K)	α (1/m)	D(T _o) m ² /s
0.36 at 244 nm	4648	806	3.3 x 10 ⁷ at 244nm	1.43 x 10 ⁻⁶
0.27 at 275 nm			1.0 x 10 ⁶ at 275 nm	

REFERENCES

1. S. Mailis , C. Riziotis, I. T. Wellington, P. G. R. Smith, C. B. E. Gawith and R. W. Eason, Direct ultraviolet writing of channel waveguides in congruent lithium niobate single crystals, *Optics Letters*, 28 (2003), 1433-1435.
2. P. Ganguly, C.L.Sones, Y.J. Ying, H. Steigerwald, K. Buse, E. Soergel, R. W. Eason, and S. Mailis, Determination of refractive indices from the mode profiles of UV-written channel waveguides in LiNbO₃-crystals for optimization of writing conditions, *J. Lightwave Technol.*, 27 (2009), 3490-3497.
3. C.L. Sones, P. Ganguly, Y.J. Ying, E. Soergel, R.W. Eason, and S. Mailis, Poling-inhibited ridge waveguides in lithium niobate crystals, *Appl. Phys. Lett.*, 97(2010), 151112-151114.
4. T. Ghosh, B. Samanta, P. C. Jana and P. Ganguly, Determination of refractive index profile and mode index from the measured mode profile of single-mode LiNbO₃-diffused waveguides, *Fiber and Integrated Optics*, 31 (2012) 1–10.
5. F. Laeri, R. Jungen, G. Angelow, U. Vietze, T. Engel, M. Wurtz, and D. Hilgenberg, Photorefraction in the ultraviolet: Materials and effects, *Appl. Phys. B*, 61(1995) 351-360.
6. M.Lax, Temperature rise induced by a laser beam," *J. Appl. Phys.*, 48 (1977) 3919-3924
7. M.Lax, Temperature rise induced by a laser beam II. The nonlinear case, *Appl. Phys. Lett.*, 33 (1978) 786-789.
8. M.Lax, in *laser solid interaction and laser processing*, edited by S. D. Ferris, H. J. Leamy and J. M. Poate (American Institute of Physics, New York (1978), p 149.
9. H. E. Cline and T. R. Anthony, Heat treating and melting material with a scanning laser or electron beam, *J. Appl. Phys.*, 48 (1977) 3895-3900
10. J. E. Moody and R. H. Hendel, Temperature profiles induced by a scanning cw laser beam, *J. Appl. Phys.*, 53 (1982) 4364-4371.
11. C. Muir, G. J. Daniell, C. P. Please, I. T. Wellington, S. Mailis and R.W. Eason, Modelling the formation of optical waveguides produced in LiNbO₃ by laser induced thermal diffusion of lithium ions, *Appl Phys A*, 83 (2006) 389-396.